# Transmission of 64-Gb/s Pilot-Assisted PAM-4 Signal Over 1440-km SSMF With Phase Noise Mitigation
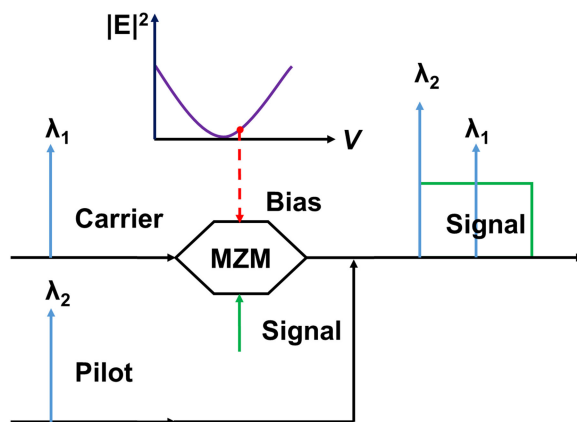
Chao Yang
Ming Luo
Cai Li
Wei Li
Xiang Li

# Transmission of 64-Gb/s Pilot-Assisted PAM-4 Signal Over 1440-km SSMF With Phase Noise Mitigation

**Chao Yang,**[1,2] **Ming Luo,**[1,2] **Cai Li,**[2] **Wei Li** [iD]**,**[1] **and Xiang Li** [iD] [3]

[1]Wuhan National Laboratory for Optoelectronics, Huazhong University of Science and Technology, Wuhan 430074, China
[2]State Key Laboratory of Optical Communication Technology and Networks, Wuhan Research Institute of Posts Telecommunications, Wuhan 430074, China
[3]National Optoelectronics Innovation Center, Wuhan Research Institute of Posts Telecommunications, Wuhan 430074, China

**Abstract:** We propose a direct detection scheme for pulse amplitude modulation (PAM) signals over long-reach fiber transmission with phase noise mitigation. In this scheme, an optical carrier is transmitted as pilot together with the optical signal, whose frequency is located at the edge of the optical signal. The electrical field of the optical signal can be retrieved via the beating between the pilot and optical signal in one photodetector at the receiver side, which facilitates the digital compensation of chromatic dispersion effect. To enable real value signal processing, digital carrier regeneration is proposed to mitigate the phase noise fluctuation in the proposed scheme. To further improve the performance, the digital signal processing including Kramers–Kronig field reconstruction and Volterra equalizer are applied to reduce the signal-to-signal beat noise and nonlinear distortions after fiber transmission. The experimental results for both 56- and 64-Gb/s PAM-4 signal transmission cases show that the performances can be significantly improvement based on the proposed scheme and DSP methods. Both 56- and 64-Gb/s PAM-4 signal transmissions over 720- and 1440-km standard single mode fiber have been successfully achieved under 7% and 20% forward error correction codes, respectively.

**Index Terms:** Direct detection, Kramers-Kronig (KK) scheme, digital carrier regeneration (DCR), Volterra equalizer.

## 1. Introduction

Nowadays, due to the fast development of mobile devices, cloud computing and big data, there is a strong demand for optical communication systems with lower cost and higher capacity. Although coherent detection techniques have been widely used in current optical transmission networks, the intensity modulation and direct detection (IM/DD) based pulse amplitude modulation (PAM) is preferred in medium/short-reach (100~300 km) datacenter interconnection and metropolitan networks due to its characteristics of low cost, simple structure and easy implementation [1]–[3]. However, the transmission distance is always limited to be less than 100 km, which is mainly

affected by the chromatic dispersion (CD) induced power fading effect. Various technologies have been proposed to eliminate the impact of CD to extend the transmission distance. Digital signal processing (DSP) technologies based on CD pre-compensation are applied to pre-distort the phase of the transmitted signal with known parameters such as transmission distance and dispersion coefficients [4]. Optical dispersion compensation module (DCM) has also been used in IM/DD link to realize real-time 56-Gb/s PAM-4 signal transmission over 100-km standard single mode fiber (SSMF) [5]. However, DCM is designed for fixed distance, which may reduce the flexibility of the optical fiber transmission networks. Recently, it has been shown that single-side band (SSB) modulation can effectively avoid the CD induced power fading by applying IQ modulator or narrow-band filtering at the transmitter side [6]. However, the direct detection scheme of SSB signal suffers from signal-to-signal beating noise (SSBN), which also degrades the system performance.

In order to mitigate the SSBN for the SSB signal based on direct detection scheme, the Kramers-Kronig (KK) receiver has been proposed [7]–[11]. The principle is that under the condition of the minimum phase, the complex electrical field can be reconstructed from its intensity which is detected by a single photodetector. Several experimental demonstrations have been reported based on KK recovery algorithm. By using KK field reconstruction or a two-stage interference cancellation scheme, a 1.6-Tb/s 8-channel WDM direct detection transmission system with virtual side-band carriers over a record distance of 1200 km Corning TXF$^{TM}$ fiber has been achieved [12]. Furthermore, single-lane 112-Gbit/s SSB modulated PAM-4 signal transmission with dual-drive Mach-Zehnder modulator (MZM) over 80-km SSMF has been realized based on bandwidth pre-compensation and KK recovery [13].

Another issues regarding the direct detection of PAM signal is the power of optical carrier occupies most of the PAM signal power, which reduces the effective optical signal-to-noise ratio. Therefore, the bias point of Mach-Zehnder modulator (MZM) can be adjusted around the null point (NP) to reduce the power of carrier signal for power efficient transmission. However, changing the bias point makes it hard to recover the signal by modulo operation after KK receiver. Recently, we have proposed digital carrier regeneration (DCR) method to solve this problem, which can effectively eliminate the influence of phase noise for discrete multi-tone (DMT) signal [14]. It is also shown that this method is compatible with the DSP steps for conventional intensity modulation schemes.

In this paper, we propose a pilot-assisted direct detection scheme for PAM-4 signal, which can transmit more than 1000-km. DCR is then first applied to PAM-4 signal when the bias point of MZM is set around NP. In addition, KK field reconstruction and Volterra equalization is applied to further improve the system performance. Compared to the standard PAM scheme, only one additional optical source is required at the transmitter side without changing other devices and structure in the conventional direct detection link. Therefore, most components in conventional direct detection PAM scheme can be re-used in our proposed scheme, which maintains the simple and cost-effective characteristics. The experimental results indicate that the proposed DSP methods greatly increase the transmission distance of PAM signals, which can satisfy the metro and inter-data center communication scenarios. The experimental results show that 64-Gb/s PAM-4 signal is successfully transmitted over 1440-km SSMF at the 20% soft-decision forward error correction (SD-FEC) threshold of $2 \times 10^{-2}$, and 56-Gb/s PAM-4 signal can achieve transmission distance of 720 km at the 7% hard-decision forward error correction (HD-FEC) threshold of $3.8 \times 10^{-3}$.

## 2. Principle

The scheme of the proposed PAM-4 signal transmission system at the transmitter side is shown in Fig. 1. The optical pilot is transmitted together with the optical signal by setting the bias point of MZM near the NP. To satisfy the minimum phase condition of KK detection technique, the pilot is located at the edge of the PAM-4 signal, and the frequency offset is $\Delta f$. After direct-detection at the
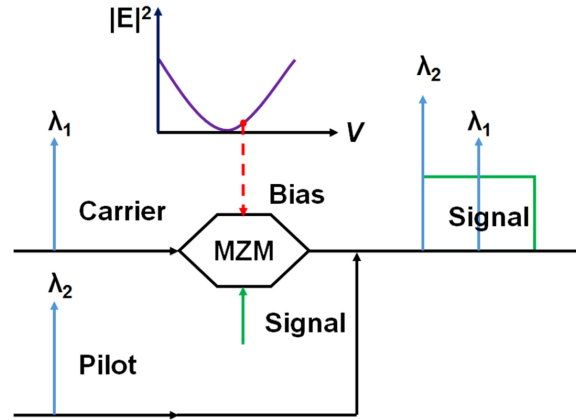
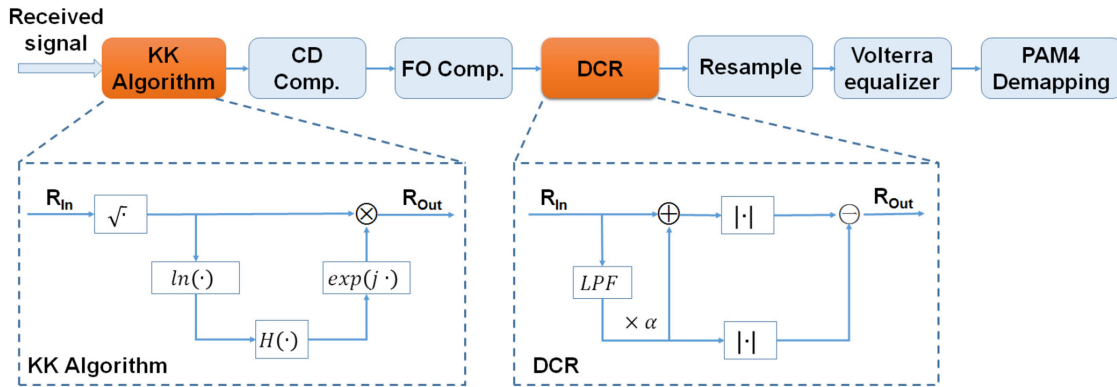Fig. 1. The scheme of the proposed PAM-4 signal at the transmitter.



Fig. 2. Schematic diagram of received signal processing for the proposed IM/DD-based PAM-4 transmission system.

receiver side, the digital received signal can be expressed as:

$$
\begin{aligned}
r(n) &= \left| A_p + (A_c + s(n))\, e^{j(2\pi \Delta fn + \Delta\varphi(n))} \right|^2 \\
&= \left| A_p \right|^2 + \left| A_c + s(n) \right|^2 \\
&\quad + A_p \cdot (A_c + s(n))\, e^{j(2\pi \Delta fn + \Delta\varphi(n))} + A_p \cdot (A_c + s(n))\, e^{-j(2\pi \Delta fn + \Delta\varphi(n))}
\end{aligned}
\tag{1}
$$

where $s(n)$ is the transmitted signal, $A_p$ and $A_c$ is the constant amplitude of the optical pliot and the optical carrier, $\Delta\varphi(n)$ represents the phase difference between the optical carrier and the pliot at the $n_{th}$ sampling point. The received electrical signal is consisted of four components: $|A_p|^2$ is the beating of the pliot, $|A_c + s(n)|^2$ is the SSBN, $A_p \cdot (A_c + s(n))e^{j(2\pi \Delta fn + \Delta\varphi(n))}$ and $A_p \cdot (A_c + s(n))e^{-j(2\pi \Delta fn + \Delta\varphi(n))}$ denote the right and left sideband signals. From Eq. (1), we can see that the SSBN contains the term of beating between the optical carrier and optical signal. Therefore, the SSBN is large if the bias point is set at the linear point (LP).

The DSP procedures for the received PAM-4 signal are presented in Fig. 2. To recover the electrical field, we employ KK detection technique. As shown in the inset of the Fig. 2, the operation
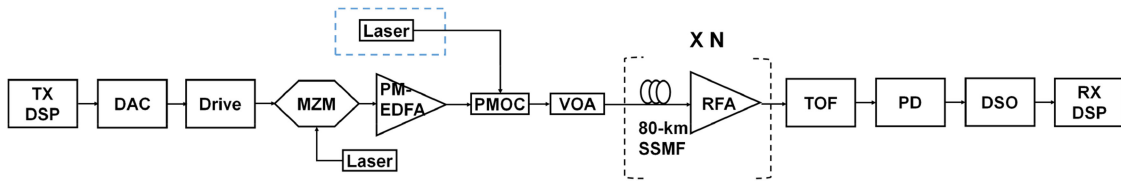
Fig. 3. Experimental setup for the fiber transmission of PAM-4 signal based on MZM with direct detection. DAC: Digital to analog converter. MZM: Mach-Zehnder modulator. PM-EDFA: polarization-maintained Erbium doped fiber amplifier. PMOC: Polarization-maintained optical coupler. VOA: Variable optical attenuator. SSMF: Standard single-mode fibre. RFA: Raman fiber amplifier. TOF: Tunable optical filter. PD: Photodetector. DSO: Digital sampling oscilloscope.

process of the algorithm is depicted as the following equations [13]:

$$h(n) = \sqrt{r(n)} \tag{2}$$

$$\varphi(n) = \mathcal{F}^{-1}\{i \cdot sign(\omega)\mathcal{F}\{ln[|h(n)|]\}\} \tag{3}$$

$$r_{KK}(n) = h(n) \cdot exp\{i\varphi(n)\} \tag{4}$$

where $r(n)$ is the detected signal, $sign(\omega)$ is the sign function, $\mathcal{F}$ and $\mathcal{F}^{-1}$ are the Fourier and inverse Fourier transform operators.

As shown in Fig. 1, the optical signal may suffer from severe laser phase noise if the bias point is set near the NP. It is noted that in conventional channel equalization for PAM signal suffering from phase noise, modulus operation is applied to eliminate the phase noise. In order to solve this problem when the bias point is setting near the NP, we apply DCR method to PAM signals after CD compensation, frequency offset compensation and DC removing, as shown in Fig. 2, the operation principle of DCR can be expressed as:

$$\begin{aligned} r_{DCR\_out}(n) &= |r_{DCR\_in}(n) + \alpha \cdot c(n)| - |\alpha \cdot c(n)| \\ &= |(\alpha + 1) \cdot A_c + s(n)| - |\alpha \cdot A_c| \\ &= A_c + s(n), \alpha > threshold \end{aligned} \tag{5}$$

where $c(n) = A_c \cdot e^{j(\Delta\varphi(n) + \Delta\theta(n))}$ is the suppressed optical carrier, which is extracted from $r_{DCR\_in}(n)$ by a narrow digital low pass filter (LPF), and $\alpha$ is amplifying factor, which makes $(\alpha + 1) \cdot A_c + s(n) > 0$. Theoretically, if $A_c \neq 0$, the signal can be recovered through DCR, as long as $\alpha$ is large enough. However, the amplifying factor $\alpha$ also amplify the in band noise of low pass filter, which will reducing system performance if $\alpha$ is too large. Therefore, the optimal value of $A_c$ should be optimized. It is noted there is a small offset between the bias point and NP in the proposed scheme, as shown in Fig. 1. This is mainly because if the carrier is too small, $\alpha$ will be too large during signal recovery process in DCR, which will amplify the in-band noise of low pass filter and result in large laser phase noise.

Then, the Volterra equalization is performed to compensate both the linear or nonlinear distortions in the transmission link. The memory lengths of the 1st, 2nd and 3rd Volterra kernels are set to be 17, 3 and 2, corresponding to the number of channel coefficients of 98 in total. Finally, the recovered signals are de-mapped to recover the original binary stream.

## 3. Experimental Setup

The experimental setup for the SSMF transmission of PAM-4 signal based on the proposed pilot-assisted scheme is shown in Fig. 3. The system setup is almost the same as the standard PAM system, and only one additional optical source is used as assisted pilot at the transmitter side. First, a pseudo random binary sequence (PRBS) with length of $2^{17}-1$ is first mapped to PAM-4 format. The PAM-4 signal is then send to a Keysight arbitrary waveform generator (AWG) M8195A, running
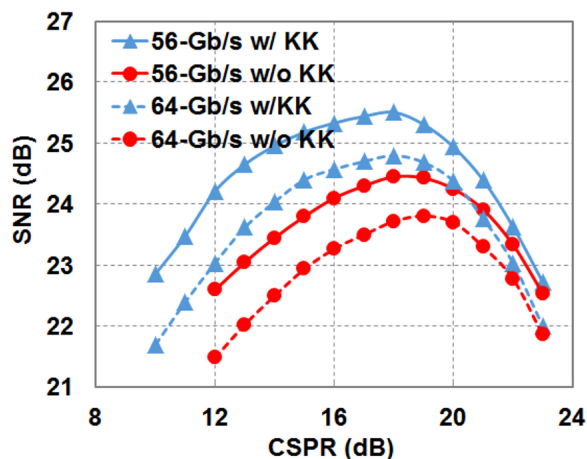
Fig. 4. SNR versus frequency spacing between pilot and optical signal for both 56-Gb/s PAM-4 signal and 64-Gb/s PAM-4 signal.

at 28-GSa/s or 32-GSa/s with electrical bandwidth of 25-GHz. The driver with bandwidth of 38-GHz is used to amplify the signal before injecting into the MZM. The electrical bandwidth of the MZM is around 40-GHz. The optical source is an Agilent external cavity laser (ECL) with 100-kHz linewidth, whose operation wavelength is set at around 1550.1-nm. The modulated optical signal is then amplified by a polarization-maintained erbium doped fiber amplifier (PM-EDFA), which is also used to control the carrier-to-signal power ratio (CSPR). By employing a polarization-maintained optical coupler (PMOC), the modulated signal is combined with the output of a second ECL whose carrier frequency is shifted by a certain frequency with respect to the first ECL. Then, a variable optical attenuator (VOA) is used to control the launch power for the combined signal. The transmission link consists of many SSMF spans without inline dispersion compensation. The length of each span is 80 km, and the loss of each span is 17 dB, which can be fully compensated by a Raman fiber amplifier (RFA).

After fiber transmission, a tunable optical filter (TOF) with the bandwidth of 100 GHz is used to eliminate the out of band noise at the receiver side. The signals are then detected by a photodetector with a bandwidth of 38-GHz. After optical-to-electrical conversion, the analog signal is then collected by a digital sampling oscilloscope (DSO) operating at 160-GSa/s with a cutoff frequency of 59-GHz and processed offline.

## 4. Results and Discussion

We first investigate the performance in the optical back-to-back (OBTB) case. In order to describe the quality of the recovered signal better, we define signal-to-noise ratio (SNR) as:

$$SNR_{dB} = 10 \cdot log_{10} \frac{S^2}{(S_R - S)^2} \tag{6}$$

where $S_R$ is the recovered signal, and $S$ is the transmitted PAM-4 signal. Fig. 4 shows the performances of SNR versus CSPR with and without KK recovery algorithm for both 56-Gb/s and 64-Gb/s PAM-4 signals at a fixed frequency spacing 22-GHz and 23-GHz under the optimal bias condition, respectively. It is observed that the performance improvements of KK recovery algorithm reduce with the increase of CSPR. Both 56-Gb/s and 64-Gb/s PAM-4 signals have the same optimal CSPR with KK recovery algorithm. Under the optimal CSPR of 18 dB, SNR improvement of 1.05 dB and 1.08 dB for 56-Gb/s and 64-Gb/s signals are achieved, when compared with the case without KK recovery algorithm. It is noted that the optimal CSPR in the proposed method is a bit larger than
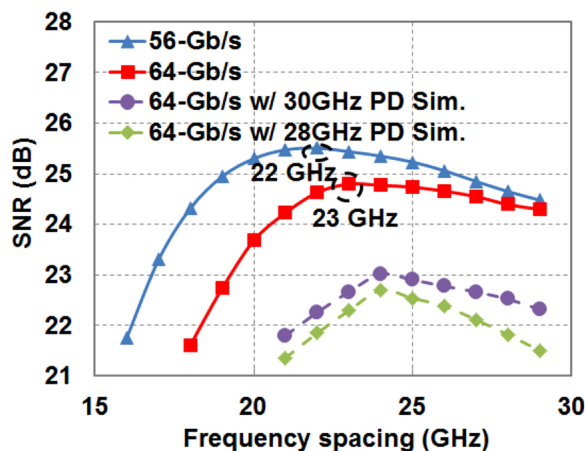
Fig. 5. SNR versus frequency spacing between pilot and optical signal for both 56-Gb/s and 64-Gb/s signals.
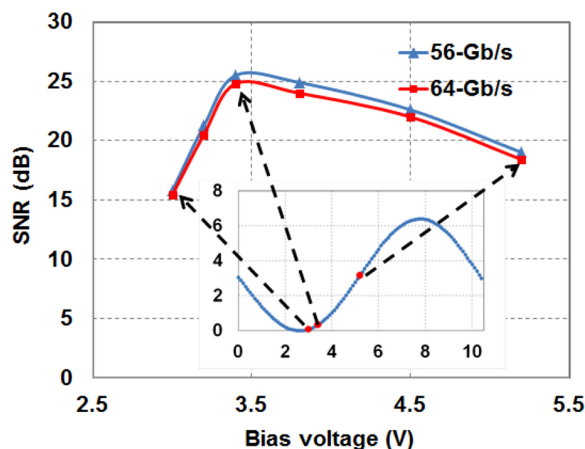


Fig. 6. SNR versus Bias voltage under the condition of optimal frequency spacing and optimal CSPR for both 56-Gb/s and 64-Gb/s signal.

that of other reported KK detection scheme. This is mainly because the SSBN is larger when the SSBI is illustrated as $|A_c + s(n)|^2$ instead of $|s(n)|^2$ according to Eq. (1).

We also study the effects of the frequency spacing between signal carrier and assisted pilot on the SNR performance under the optimal CSPR of 18-dB in the optical back-to-back (OBTB) case. As shown in Fig. 5, when the frequency spacing is small, the crosstalk of the assisted pilot to the PAM-4 signal may degrade the system performance. When the frequency spacing exceeds the optimal value, the SNR will also reduce, due to limited bandwidth of the PD. The results for 64-Gb/s PAM-4 signals after low-pass filter with bandwidth of 28-GHz and 30-GHz are also shown in Fig. 5 to emulate the cases when the bandwidth of PD is low. It is indicated that the performance of the system is degraded if a low-bandwidth PD is used. The optimal value of frequency spacing is 22 GHz and 23 GHz for 56-Gb/s and 64-Gb/s PAM-4 signals, respectively. It is also noted that the performance degradation is less than 1 dB even if the frequency spacing is shifted by ±2 GHz. Therefore, the proposed scheme has certain robustness against frequency drifting.

Then, we investigate the impact of bias voltage of the MZM on the performance of the system. Fig. 6 shows the performances of SNR versus bias voltage for both 56-Gb/s and 64-Gb/s PAM-4 signals, respectively. It is observed that the optimal Bias is 3.4-V, which is closer to NP than LP
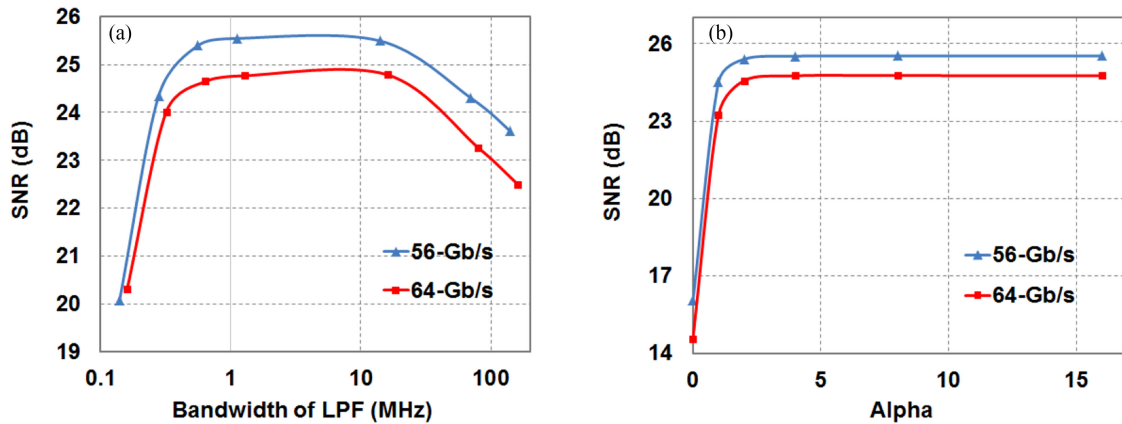
Fig. 7. (a) SNR versus LPF bandwidth and (b) SNR versus amplifying factor of DCR for both 56-Gb/s and 64-Gb/s signal.
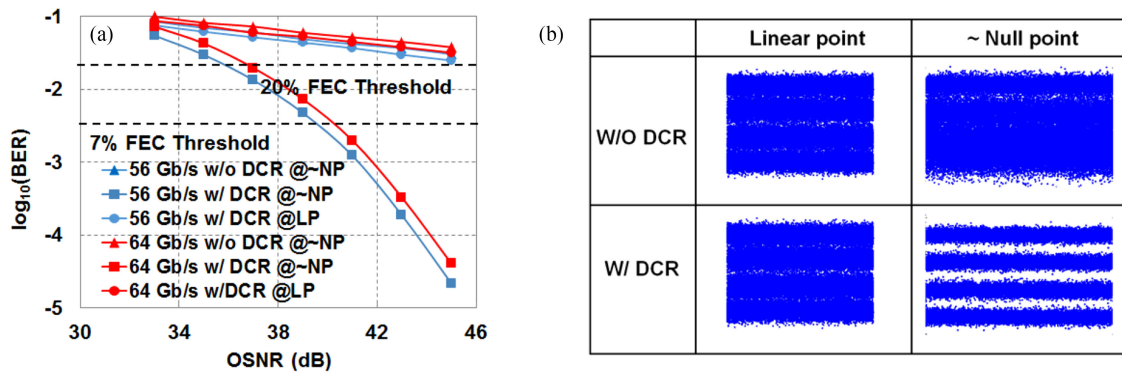


Fig. 8. (a) BER versus OSNR for 56-Gb/s and 64-Gb/s signals when MZM is biased at LP and ~NP at LP and ~NP with and without DCR in OBTB case. (b) Waveforms of recovered signal when MZM is biased at LP and ~NP with and without DCR.

as illustrated in the inset of the Fig. 6. The experimental results are consistent with the theoretical deduction mentioned earlier.

We also study the effects of the parameters of DCR algorithm on the SNR performance in the cases of OBTB under all optimal conditions. Fig. 7(a) shows the BER versus different LPF bandwidth of DCR. We can see that the optimal LPF bandwidth is at least 1-MHz. It can be explained that LPF bandwidth of DCR must contains the entire suppressed optical carrier. However, the bandwidth is limited to a certain range (<10-MHz) to avoid additional noise. At the same time, the effects of the amplifying factor is also investigated. As shown in the Fig. 7(b), with the increase of amplifying factor, the SNR of the system tends to a constant value and remains unchanged. As long as $\alpha$ is large enough, which makes $(\alpha + 1) \cdot A_c + s(n) > 0$, increasing $\alpha$ will not change the system performance.

Figure 8(a) shows the received BER as a function of OSNR under the condition of optimal frequency spacing and CSPR in the OBTB case. Since the measured OSNR contains the assisted pilot, the value of OSNR is much larger than that of conventional PAM signal. Under this condition, The OSNR threshold for the 7% HD-FEC and 20% SD-FEC are 39.5-dB and 37-dB for 56-Gb/s and 64-Gb/s PAM-4 signals, respectively. It is also shown in Fig. 8(a) that the performances can be greatly improved when DCR is applied for phase recovery. The performance improvement of DCR is mainly due to the fact that modulo operation can be applied to the received signal, which mitigates the effect of phase noise in the proposed scheme. It is also noted in Fig. 8(a) that the system is affected by the phase noise only when the bias point is near the NP. Therefore, the DCR may have no effect on the system performance when the MZM is biased at the LP. As also indicated
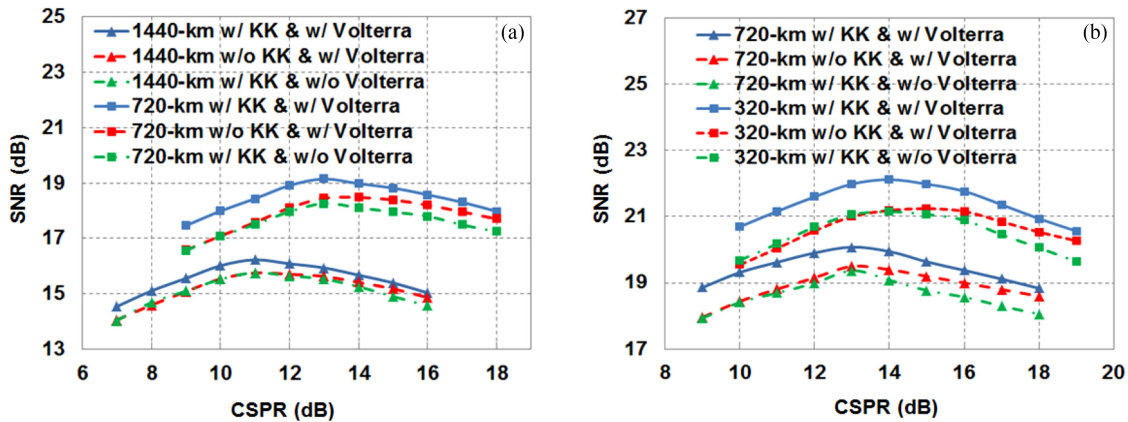
Fig. 9. SNR versus CSPR with and without KK algorithm after SSMF transmission for (a) 56-Gb/s and (b) 64-Gb/s PAM-4 signals.
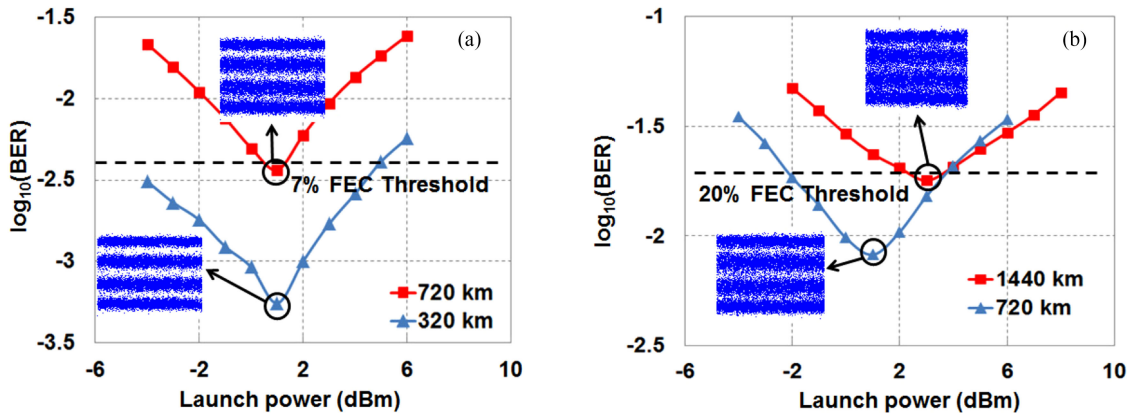


Fig. 10. BER versus launch power for different transmission distance for (a) 56-Gb/s PAM-4 signals, and (b) 64-Gb/s PAM-4 signals.

in Fig. 8(b) for 56-Gb/s PAM-4 signal, performance improvement is only observed when the MZM is biased near the NP.

Then, we investigate the transmission performance of the PAM-4 signal over SSMF transmission based on the proposed scheme. Fig. 9 shows the performances of SNR versus CSPR with and without KK recovery algorithm after different transmission distance. Similar to OBTB case, with the increase of CSPR, the improvement of SNR brought by KK recovery algorithm is gradually reduced. It is noted that with longer transmission distance, the SNR of the received signal is reduced, and the optimal value of CSPR is increased. For 56-Gb/s PAM-4 signals, the optimal value of CSPR after 720 km and 320 km SSMF transmission are 14 dB and 13 dB, respectively. The corresponding SNR improvements brought by KK recovery algorithm are 0.7 dB and 1.0 dB, respectively. For 64-Gb/s PAM-4 signals, the optimal value of CSPR after 1440 km and 720 km SSMF transmission are 13 dB and 11 dB, with corresponding SNR improvements of 0.5 dB and 0.8 dB, respectively. From Fig. 9, we can also see that Volterra series based nonlinear equalization shows better performance than the conventional linear channel equalization method.

Figure 10 shows the BER versus launch power for different transmission distance. We can see that the optimal launch power for both 720-km and 320-km transmission is 1 dBm for 56-Gb/s PAM-4 signals. However, the optimal launch power is 1 dBm and 3 dBm for the 1440-km and 720-km transmission for 64-Gb/s PAM-4 signals, respectively. The BER are $3.6 \times 10^{-3}$ over 720-km transmission and $1.8 \times 10^{-2}$ over 1440-km SSMF transmission for the 56-Gb/s and 64-Gb/s

PAM-4 signals under the optimal value of launch power, which are below the corresponding 7% and 20% FEC thresholds. It is noted that when the transmission distance is 320-km, the BER of 56-Gb/s PAM-4 signal is $5.5 \times 10^{-4}$, which can satisfy the requirements for datacenter interconnection based on low-complexity FEC with hard decision.

## 5. Conclusions

We propose a pilot-assisted scheme base on MZM and direct detection to extend the fiber transmission distance. The bias point of MZM is set near the null point for power efficient transmission with reduced SSBN. DCR is proposed to mitigate the effect of laser phase noise based on the proposed scheme. With the help of KK field reconstruction, DCR and Volterra equalization, 56-Gb/s and 64-Gb/s PAM-4 signal transmission over 720-km and 1440-km SSMF can be successfully achieved. The proposed method can effectively improve the transmission distance by reusing the conventional structure of IM/DD system with only one additional laser source, which is thought to be feasible in future low-cost short-reach optical fiber applications.

## References

[1] K. Zhong, X. Zhou, J. Huo, C. Yu, C. Lu, and A. P. T. Lau, "Digital signal processing for short-reach optical communications: A review of current technologies and future trends," *IEEE/OSA J. Lightw. Technol.*, vol. 36, no. 2, pp. 377–400, Jan. 2018.

[2] A. G. Reza and J. K. K. Rhee, "Nonlinear equalizer based on neural networks for PAM-4 signal transmission using DML," *IEEE Photon. Technol. Lett.*, vol. 30, no. 15, pp. 1416–1419, Aug. 2018.

[3] X. Pang *et al.*, "Experimental study of 1.55-$\mu$m EML-based optical IM/DD PAM-4/8 short reach systems," *IEEE Photon. Technol. Lett.*, vol. 29, no. 6, pp. 523–526, Mar. 2017.

[4] A. Masuda, S. Yamamoto, Y. Sone, S. Kawai, and M. Fukutoku, "112-Gb/s C-band transmission using 4-level/7-level coding PAM with chromatic-dispersion pre-compensation under 25-GHz bandwidth-limitation," in *Proc. Opt. Fiber Commun. Conf. Exhib.*, Mar. 2017, pp. 1–3.

[5] N. Eiselt *et al.*, "First real-time 400 G PAM-4 demonstration for inter-data center transmission over 100 km of SSMF at 1550 nm," in *Proc. Opt. Fiber Commun. Conf. Exhib.*, Mar. 2016, pp. 1–3.

[6] Q. Zhang *et al.*, "Single-lane 180 Gb/s SSB-duobinary-PAM-4 signal transmission over 13 km SSMF," in *Proc. Opt. Fiber Commun. Conf. Exhib.*, Mar. 2017, pp. 1–3.

[7] A. Mecozzi, C. Antonelli, and M. Shtaif, "Kramers–Kronig coherent receiver," *OSA Optica*, vol. 3, no. 11, pp. 1220–1227, Nov. 2016.

[8] Z. Li *et al.*, "Spectrally efficient 168 Gb/s/λ WDM 64-QAM single-sideband nyquist-subcarrier modulation with Kramers–Kronig direct-detection receivers," *IEEE/OSA J. Lightw. Technol.*, vol. 36, no. 6, pp. 1340–1346, Mar. 2018.

[9] M. Presi *et al.*, "Transmission in 125-km SMF with 3.9 bit/s/Hz spectral efficiency using a single-drive MZM and a direct-detection Kramers-Kronig receiver without optical CD compensation," in *Proc. Opt. Fiber Commun. Conf. Exhib.*, Mar. 2018, pp. 1–3.

[10] Z. Li *et al.*, "SSBI mitigation and Kramer-Kronig scheme in single-sideband direct-detection transmission with receiver-based electronic dispersion compensation," *IEEE/OSA J. Lightw. Technol.*, vol. 35, no. 10, pp. 1887–1893, May 2017.

[11] X. Chen *et al.*, "218-Gb/s single-wavelength, single-polarization, single-photodiode transmission over 125-km of standard single-mode fiber using Kramers-Kronig detection," in *Proc. Opt. Fiber Commun. Conf. Exhib.*, Mar. 2017, pp. 1–3.

[12] S. T. Le, K. Schuh, F. Buchali, M. Chagnon, and H. Bülow, "1.6 Tbps WDM direct detection transmission with virtual-carrier over 1200 km," in *Proc. Opt. Fiber Commun. Conf. Exhib.*, Mar. 2018, pp. 1–3.

[13] L. Shu *et al.*, "Single-Lane 112-Gbit/s SSB-PAM4 transmission with dual-drive MZM and Kramers–Kronig detection over 80-km SSMF," *IEEE Photon. J.*, vol. 9, no. 6, Dec. 2017, Art. no. 7204509.

[14] C. Li, R. Hu, Q. Yang, M. Luo, W. Li, and S. Yu, "Fading-free transmission of 124-Gb/s PDM-DMT signal over 100-km SSMF using digital carrier regeneration," *OSA Opt. Exp.*, vol. 24, no. 2, pp. 817–824, Jan. 2016.